Study of Injection and Retention of Charges in Silica-Based Nanocomposite Dielectrics: Impact of Size of Silver Nanoparticles

Sariette Nowa-Tatchum, Christina Villeneuve-Faure, Laurent Boudou, Kremena Makasheva

Study of injection and retention of charges in silica-based nanocomposite dielectrics: impact of size of silver nanoparticles

Sariette Nowa-Tatchum, Christina Villeneuve-Faure*, Laurent Boudou and Kremena Makasheva

LAPLACE (Laboratoire Plasma et Conversion d'Energie), Université de Toulouse, CNRS, UT3, INPT, Toulouse, France

*email address of corresponding author villeneuve@laplace.univ-tlse.fr

***Abstract*—It is well-known that dielectric materials store charges when they are subjected to an electric field. Recently, nanocomposite materials were identified as promising candidates to tune this effect. This study focuses on silica-based nanocomposites containing a single plane of silver nanoparticles (AgNPs) embedded at 5 nm under the surface. More particularly, the influence of AgNPs size on charges injection and retention is investigated. The electrical charges are injected locally by using an Atomic Force Microscopy (AFM) tip and the related surface potential profile is probed by Kelvin Probe Force Microscopy (KPFM). The results show that proper selection of the size of AgNPs allows a fine control of the charges dynamics.**

Keywords*— *nanocomposite dielectric layers, charges injection, Kelvin Probe Force Microscopy, silver nanoparticles, plasma deposition

I. INTRODUCTION

Dielectric materials are characterized by their capacity to store charges when subjected to an electric field. However, this property is the main source of failure of Micro ElectroMechanical Systems (MEMS) [1] or microelectronic devices [2]. An emerging solution involves the use of nanostructured dielectric layers to control charges injection and transport in thin dielectric films, therefore offering new perspectives for the reliability and performance of electronic devices [3]. An example of such nanostructured dielectrics is a thin silica (SiO_2) layer containing a plane of metallic (silver) nanoparticles (AgNPs), embedded beneath the surface. Besides, a deep understanding of the physical mechanisms underlying charges injection and transport at the nanoscale is needed. Investigation of thin dielectric layers by application of classical non-destructive techniques for probing space charges distributions in insulators, such as pulsed electro acoustic (PEA) [4] or focused laser intensity modulation method (FLIMM) [5] becomes unsuitable due to the required minimum dielectric thickness (no less than a few tens of micrometers). Thus, electrical modes derived from Atomic Force Microscopy (AFM) come to the fore. They offer the possibility to inject charges locally and to probe the resulting modifications in the electrostatic field at the nanoscale level.

In this paper, we use Kelvin Probe Force Microscopy (KPFM) to probe modification of the surface potential distribution in AgNPs-based nanocomposites (NCs) due to the trapped charges. This choice is based on the good KPFM spatial resolution (around 10 nm) and its high sensitivity to trapped charges [6]. The aim is to study the mechanisms of charges injection and retention in these dielectric structures, as well as to assess the influence of AgNPs size on these mechanisms.

II. EXPERIMENTAL METHODOLOGY

A. Plasma deposition of nanostructured layers

Schematic representation of the investigated NC structures is given in Fig. 1. The NCs contain a single plane of AgNPs embedded in a thin silica layer close to the surface. For differential analyses a SiO_2 layer alone (without AgNPs) is considered as well.

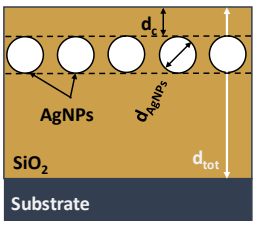

Figure 1. Structure of a nanocomposite containing a plane of AgNPs embedded in SiO_2 layer beneath the surface.

A plasma process based on an axially-asymmetric radiofrequency capacitively-coupled discharge, maintained at low gas pressure in argon, was applied for the NCs synthesis [3], [7]. It successfully combines in the same reactor plasma polymerization of hexamethyldisiloxane (HMDSO, $Si_2O(CH_3)_6$) and oxygen (O_2) as precursors to deposit the SiO_2 layers and metallic sputtering of a silver target to deposit the AgNPs. All samples were deposited on Si-substrates. Two sizes of AgNPs (d_{AgNPs}, Fig. 1) in the range 5 – 20 nm were selected for this study. The NC elaboration process was performed in three steps: 1) deposition of a silica layer – named base, 2) synthesis of AgNPs and 3) deposition of a second silica layer – named cover layer (d_c) that fixes the in-depth position at which the AgNPs are embedded in the silica layer [3]. The total thickness of the NC structures – noted d_{tot} – is kept the same for all samples to advantage the analyses.

B. Structural characterization

NCs were characterized by spectroscopic ellipsometry (SE) with a Semilab SE-2000 ellipsometer in the 250 – 850 nm spectral range with an incident angle of 75°. The Forouhi-Bloomer dispersion law was applied to extract the thickness and the optical properties of the silica layers. NCs morphological characterization (AgNPs size, surface density and localization) was performed with Transmission Electron Microscopy (TEM) by a JEOL JEM 2100F microscope.

C. Electrical characterization procedure

Charges injection and decay were performed with a Bruker Multimode 8 apparatus using a three steps method. First, each

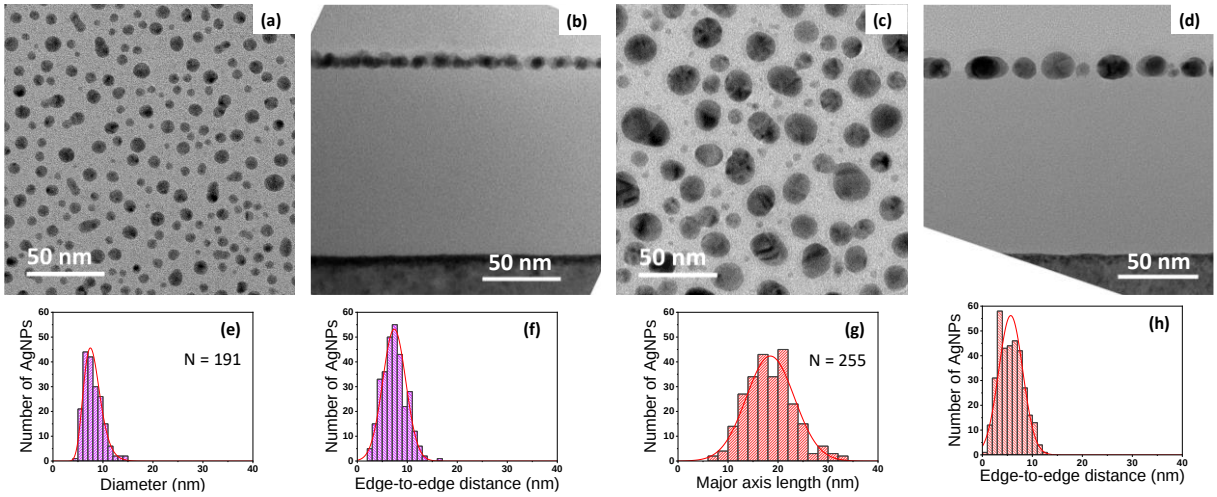

Figure 2. TEM images of the AgNPs-based NCs (first row): small AgNPs < 10 nm in size (a) plane view, (b) cross–section view and large AgNPs, (c) plane view, (d) cross-section view, and statistical analysis (second row): (e) diameter of small AgNPs, (f) edge-to-edge distance between the small AgNPs, (g) major axis of large AgNPs and (h) edge-to-edge distance between the large AgNPs.

sample (NCs or SiO_2 alone) was conditioned at 110°C for 5 min to eliminate the water film on the sample surface and then placed in an environmentally controlled chamber, maintained under a nitrogen (N_2) atmosphere. Secondly, charges were injected in contact mode (contact force around 30 nN) using a PtIr-coated silicon AFM tip (curvature radius R_c = 27 nm, spring constant $k \approx 3$ N/m and resonant frequency $f_0 \approx 75$ kHz). Positive or negative DC bias V_0 ranging from −40 to +40 V (step of 10 V) was applied to the AFM tip for 1 min, the sample back side remained grounded. Finally, surface potential was measured through Amplitude Modulation (AM) KPFM in lift mode (10 nm-lift).

III. RESULTS AND DISCUSSION

A. *Structural properties of AgNPs-based nanocomposites*

Figure 2 shows TEM images of the studied NCs in plane and cross-section views for AgNPs of small (Figs. 2(a) and (b)) and large (Figs. 2(c) and (d)) sizes. Regardless their size, the AgNPs appear randomly distributed in the plane (Figs. 2(a) and (c)), which is consistent with previous studies carried out by AFM [8]. In the two cases, the AgNPs are organized in a monolayer, embedded at d_c = 5.0 nm beneath the silica surface (Figs. 2(b) and (d)). The total thickness of all samples is d_{tot} = 135 nm.

After dimensional analysis, one finds an average size of 8.0 ± 1.8 nm and 18.5 ± 4.8 nm for the small (following a lognormal distribution) and large (following a normal distribution) AgNPs, respectively (Figs. 2(e) and (g)). Moreover, the interparticle distance decreases with the average size: from 7.4 ± 2.3 nm (small AgNPs) to 5.6 ± 2.5 nm (large AgNPs) (Figs. 2(f) and (h)). This implies that the surface density decreases with AgNPs size, from 6.1×10^{11} NPs/cm^2 (covered area of 29.6 %) for small AgNPs to 1.7×10^{11} NPs/cm^2 (covered area of 38.0 %) for large AgNPs. The shape of AgNPs is spherical for the small AgNPs (Fig. 2(a)) with a tendency of evolution towards a prolate spheroid for the large AgNPs (Fig. 2(c)), with an eccentricity of ε_c = 0.5 for the latter. However, with such low level of eccentricity, the large AgNPs can still be considered spherical.

B. *Effect of AgNPs size on charges injection*

After charges injection the surface topography (Fig. 3(a)) and the surface potential (Fig. 3(b)) were probed. Comparison of surface topography and surface potential maps demonstrates that the trapped charges have no impact on the surface topography, while they appear as a circular spot on the surface potential map. The surface potential profile corresponding to a cut along the dotted red line is presented on Fig. 3(c). In order to go further on the analysis, this profile is fitted with a Gaussian function to extract two parameters: the surface potential maximum V_m and the peak full width at half maximum (FWHM) which represents the lateral spreading of injected charges. To assess the impact of AgNPs size on the charges injection the evolution of V_m and FWHM as a function of applied DC bias V_0 was followed (Fig. 4). Whatever the AgNPs size, the maximum of the surface potential V_m increases with the applied voltage V_0 in a similar way (Fig. 4(a)). The FWHM increases with V_0 for both polarities, which suggests similar lateral spreading mechanisms for both carriers: electrons and holes (Fig. 4(b)). These results are close to those previously reported in the literature for such NCs [9]. For a fixed V_0, the FWHM increases with the AgNPs size, which implies that the charges spreading is highly sensitive to the AgNPs size and interparticle distance.

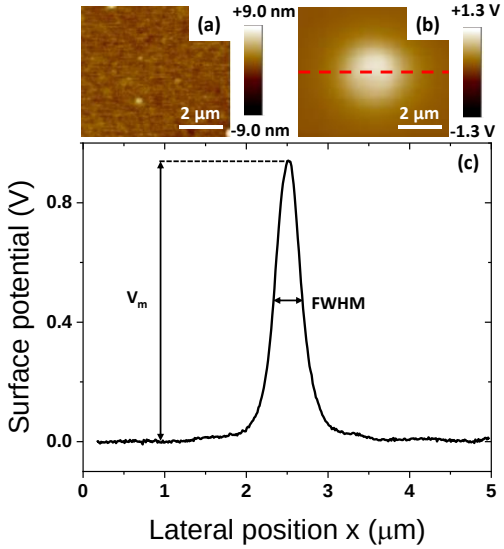

Figure 3. (a) Surface topography, (b) potential distribution and (c) profile of the surface potential after injection at 20 V for 1 min in SiO_2.

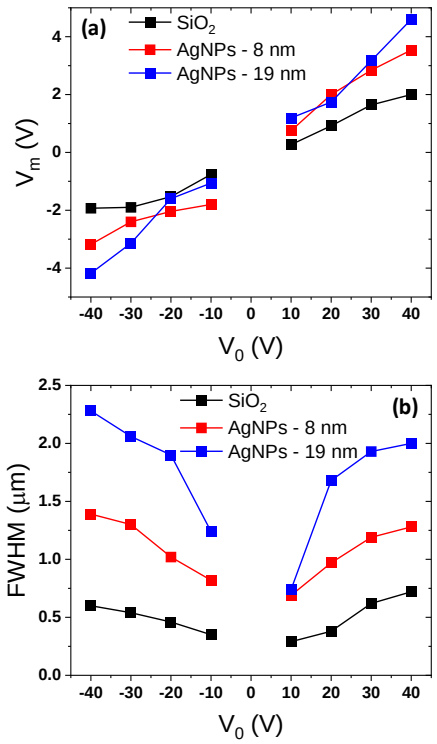

Figure 4. Evolution of (a) surface potential maximum and (b) FWHM with the applied bias for the different NC structures and SiO_2.alone.

As far as the injection mechanism in the NCs is concerned, our reasoning is as follows: applying a bias to a dielectric material reduces the Schottky barrier, which leads to charges injection from the electrode (AFM tip) to the material (NCs). Given the very small depth at which the AgNPs are embedded in the silica layer (d_c = 5 nm), it's possible to assume that, via tunneling, the injected charges are transported to the AgNPs and stored there [10]. So, the AgNPs can be considered as charges traps. The trapped charges generate a higher surface potential and consequently increase the charges injection.

C. Injected charges dynamic

To investigate charges dynamic after injection at -20V for 1 min, surface topography (Fig. 5(a)) and surface potential maps (Figs. 5(b)-(e)) were acquired at different times. As for SiO_2, shown in Fig. 3(a), the surface topography is not impacted by the injected charge in the NCs (Fig. 5(a)). The evolution of surface potential spot with time is characterized by a decreasing of the surface potential (loss of contrast) and an increasing of the lateral dimension of the potential spot on the maps (highlighted by dash lines). The spot size here is taken at the wings level of the corresponding potential profile.

As for the charges injection, the injected charges dynamics was quantified by following the evolution of the same two parameters, V_m and FWHM, but for comparison purposes the former was normalized to the initial value of the maximum surface potential (V_{mn}) and the latter was represented by the surface potential profile broadening ΔW which corresponds to the difference between the FWHM at given time after injection and the FWHM just after injection. Figure 6 represents the evolution of the normalized surface potential maximum V_{mn} and of the profile broadening ΔW over 90 min after charges injection.

Figure 6(a) compares the evolution of V_{mn} after charge injection for the bare silica and the two NCs structures. A

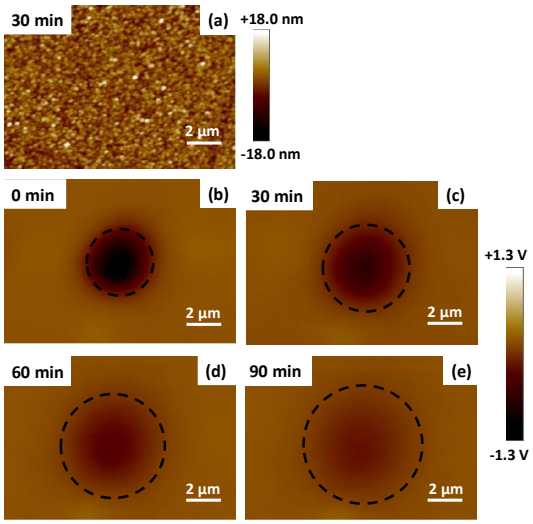

Figure 5. (a) Topography (at 30 min) and (b)-(e) Evolution of the surface potential maps at various time after charge injection at -20 V for 1 min in the NC with large AgNPs.

similar behavior is observed for SiO_2 alone and the NC with small AgNPs. The surface potential remains almost the same over time, with loss limited to less than 20% after 90 min. For the NC with large AgNPs, the decrease of the surface potential maximum is more pronounced, up to 70% after 90 min. Figure 6(b) compares the lateral broadening of the surface potential profile for silica and the two NCs. The behavior is similar to the surface potential maximum dynamic. Indeed, there is almost no expansion of the injected charges cloud in the bare silica and in the NCs with small AgNPs. For the NC with large AgNPs the surface potential broadening is more important. This implies that volume and lateral charges dynamics are strongly impacted by the AgNPs size and the interparticle distance.

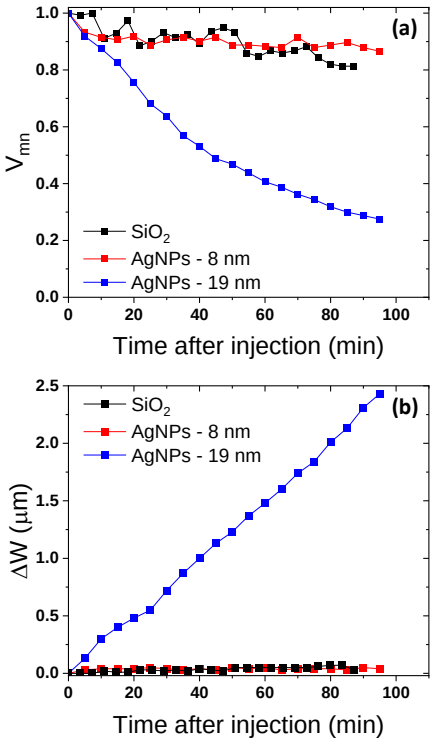

Figure 6 Evolution of (a) normalized potential maximum and (b) potential profile broadening with time for different structures.

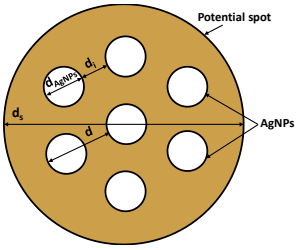

Figure 7. Illustration of the potential spot in presence of AgNPs.

Since charges spread linearly with time, the average lateral charges spreading speed could be extracted from the slope of all curves $\Delta W = f(t)$ for the bare silica and the NCs. Evaluating this slope for different applied bias V_0 permits to extract the mean value and standard deviation. The peak broadening speed is equal to 9 ± 6 nm/min for the bare SiO_2, and to 5 ± 3 nm/min, and 29 ± 8 nm/min for the NCs with small and large AgNPs, respectively. These results point to different charge dynamics in the three structures considered here: bare SiO_2 and NCs with small and large AgNPs. In the bare SiO_2 structure, the charge dynamics can be assigned to the charge traps belonging to the dielectric structure (mainly chemical traps) and in the NC with small AgNPs to the AgNPs (physical traps) and the dielectric structure. However, these two structures exhibit the same dynamic: the charges remain trapped and dissipate very slowly, mainly through volume mechanisms, featured by the limited peak broadening. When the AgNPs are large in size, the expressed charge dynamic is more complex with a combination of surface and volume dispersive mechanisms, clearly emphasized by the simultaneous decrease of the potential maximum and the increase of the peak broadening, implying that the charges lateral spreading is favored by the presence of large AgNPs.

A way to assess the impact of AgNPs of different size on the charges dynamics is to calculate the number of AgNPs involved through the time-evolution of the surface potential spot. This physical situation can be described as follows (Fig. 7): a surface potential spot of diameter d_s is measured at time t = 0s after charge injection in a NCs containing a plane of homogeneously distributed AgNPs of diameter d_{AgNPs} and interparticle distance d_i, embedded at a small depth beneath the surface. To account for the periodicity in the structure a diameter $d = d_{AgNPs} + d_i$ is introduced, which allows to calculate the area containing AgNPs (S_{AgNPs}). Considering the ratio between the potential spot area (S_p) and the one containing AgNPs, the number of AgNPs under the surface potential spot can be extracted. Performing this calculation for time t = 0s and 90 min after charges injection, we find that 12183 small AgNPs are localized under the surface potential spot just after charge injection and that this number remains almost unchanged 90 min later, for which only 582 small AgNPs are additionally involved. Increasing the size of AgNPs, which is accompanied by a decrease of the interparticle distance, leads to the following numbers: 15625 large AgNPs are localized under the surface potential spot at t = 0s and the potential spot extends over 62500 NPs in 90 min, which means that 4 times more AgNPs are involved in the charges dynamics.

IV. CONCLUSION

This work presents a study on the impact of AgNPs size on charges injection mechanisms and charges dynamics in AgNPs-based NCs thin dielectric layers. The plasma deposition method of such NCs structures enables a fine control over the structure parameters. The AgNPs are distributed homogeneously in the plane, with an interparticle distance decreasing as the size of AgNPs increases. Since the AgNPs are embedded very close to the silica surface, the charges injection process is impacted by their size. We observe that depending on the AgNPs size, the charges dissipation mechanisms vary, changing from very limited volume dissipation for small AgNPs to a combination of surface and volume dissipation when the AgNPs are large in size. This work suggests that proper selection of the AgNPs size in the plane allows a fine control over the charges dynamics of NCs dielectric structures. Further work will be directed to the description of the electric field distribution and its distortion in presence of a plane of AgNPs of different size embedded at small in-depth positions beneath the silica surface.

ACKNOWLEDGMENT

This work was supported by l'Agence Nationale de la Recherche in France, project ANR BENDIS (ANR-21-CE09-0008). The authors acknowledge support from the Centre de microcaractérisation Raymond Castaing (UAR 3623) of Université de Toulouse and thank Dr. A. Pugliara and Mr. L. Weingarten for the TEM observations.

REFERENCES

[1] G. M. Rebeiz, *RF MEMS: theory, design, and technology*. John Wiley & Sons, 2004.

[2] G. Ribes *et al.*, "Review on high-k dielectrics reliability issues," *IEEE Trans. Device Mater. Relib.*, vol. 5, no. 1, pp. 5–19, Mar. 2005, doi: 10.1109/TDMR.2005.845236.

[3] K. Makasheva *et al.*, "Dielectric Engineering of Nanostructured Layers to Control the Transport of Injected Charges in Thin Dielectrics," *IEEE Transactions on Nanotechnology*, vol. 15, no. 6, pp. 839–848, 2016, doi: 10.1109/TNANO.2016.2553179.

[4] O. Gallot-Lavallee and G. Teyssedre, "Space charge measurement in solid dielectrics by the pulsed electro-acoustic technique," in *Proceedings of the 2004 IEEE International Conference on Solid Dielectrics, 2004. ICSD 2004.*, Toulouse, France: IEEE, 2004, pp. 268–271. doi: 10.1109/ICSD.2004.1350342.

[5] A. Petre, C.-D. Pham, D. Marty-Dessus, and L. Berquez, "Three-dimensional space charge cartographies by FLIMM in electron irradiated polymers," *Journal of Electrostatics*, vol. 67, no. 2–3, pp. 430–434, May 2009, doi: 10.1016/j.elstat.2008.12.011.

[6] W. Melitz, J. Shen, A. C. Kummel, and S. Lee, "Kelvin probe force microscopy and its application," *Surface Science Reports*, vol. 66, no. 1, pp. 1–27, Jan. 2011, doi: 10.1016/j.surfrep.2010.10.001.

[7] A. Pugliara, C. Bonafos, R. Carles, B. Despax, and K. Makasheva, "Controlled elaboration of large-area plasmonic substrates by plasma process," *Mater. Res. Express*, vol. 2, no. 6, p. 065005, Jun. 2015, doi: 10.1088/2053-1591/2/6/065005.

[8] S. Nowa-Tatchun, C. Villeneuve-Faure, L. Boudou, and K. Makasheva, "Impact of Silver Nanoparticles Embedded in a Silica Layer on the Surface Morphology of the Structure: Evaluation by Atomic Force Microscopy," in *2023 IEEE 23rd International Conference on Nanotechnology (NANO)*, Jeju City, Korea, Republic of: IEEE, Jul. 2023, pp. 233–236. doi: 10.1109/NANO58406.2023.10231207.

[9] C. Villeneuve-Faure *et al.*, "Kelvin force microscopy characterization of charging effect in thin a-$SiO_x N_y$:H layers deposited in pulsed plasma enhanced chemical vapor deposition process by tuning the Silicon-environment," *Journal of Applied Physics*, vol. 113, no. 20, p. 204102, May 2013, doi: 10.1063/1.4805026.

[10] C. Djaou, C. Villeneuve-Faure, K. Makasheva, L. Boudou, and G. Teyssedre, "Analysis of the charging kinetics in silver nanoparticles-silica nanocomposite dielectrics at different temperatures," *Nano Ex.*, vol. 2, no. 4, p. 044001, Dec. 2021, doi: 10.1088/2632-959X/ac3886.